

Predicting isovector charmonium-like states from $X(3872)$ properties

Zhen-Hua Zhang^{1,2,*} Teng Ji^{3,†} Xiang-Kun Dong^{3,‡} Feng-Kun Guo^{1,2,4,5,§}
 Christoph Hanhart⁶ Ulf-G. Meißner^{3,6,7} and Akaki Rusetsky^{3,7}

¹CAS Key Laboratory of Theoretical Physics, Institute of Theoretical Physics, Chinese Academy of Sciences,
 Zhong Guan Cun East Street 55, Beijing 100190, China

²School of Physical Sciences, University of Chinese Academy of Sciences, Beijing 100049, China

³Helmholtz-Institut für Strahlen- und Kernphysik and Bethe Center for Theoretical Physics,
 Universität Bonn, D-53115 Bonn, Germany

⁴Peng Huanwu Collaborative Center for Research and Education, Beihang University, Beijing 100191, China

⁵Southern Center for Nuclear-Science Theory (SCNT), Institute of Modern Physics,
 Chinese Academy of Sciences, Huizhou 516000, China

⁶Institute for Advanced Simulation (IAS-4), Forschungszentrum Jülich, D-52425 Jülich, Germany

⁷Tbilisi State University, 0186 Tbilisi, Georgia

Using chiral effective field theory, we predict that there must be isovector charmonium-like $D\bar{D}^*$ hadronic molecules with $J^{PC} = 1^{++}$ denoted as W_{c1} . The inputs are the properties of the $X(3872)$, including its mass and the ratio of its branching fractions of decays into $J/\psi\rho^0$ and $J/\psi\omega$. The predicted states are virtual state poles of the scattering matrix, pointing at a molecular nature of the $X(3872)$ as well as its spin partners. They should show up as either a mild cusp or dip at the $D\bar{D}^*$ thresholds, explaining why they are elusive in experiments. The so far negative observation also indicates that the $X(3872)$ is either a bound state with non-vanishing binding energy or a virtual state, only in these cases the $X(3872)$ signal dominates over that from the W_{c1}^0 . The pole positions are $3865.3^{+4.2}_{-7.4} - i0.15^{+0.04}_{-0.03}$ MeV for W_{c1}^0 and $3866.9^{+4.6}_{-7.7} - i(0.07 \pm 0.01)$ MeV for W_{c1}^\pm . The findings imply that the peak in the $J/\psi\pi^+\pi^-$ invariant mass distribution is not purely from the $X(3872)$ but contains contributions from W_{c1}^0 predicted here. The states should have isovector heavy quark spin partners with $J^{PC} = 0^{++}$, 2^{++} and 1^{+-} , with the last one corresponding to Z_c . We suggest to search for the charged 0^{++} , 1^{++} and 2^{++} states in $J/\psi\pi^\pm\pi^0$.

Introduction.—One of the prevailing mysteries in the realm of strong interaction physics is connected to the internal composition of the XYZ states observed by various experiments in the heavy quarkonium mass range (for reviews, see Refs. [1–9]). A profound comprehension of this matter could illuminate the distribution of energy excitation within the nonperturbative domain of quantum chromodynamics (QCD). Specifically, it could reveal what kind of clustering (if any) emerges within multi-quark states. For example, it could determine whether the quarks cluster into individual hadrons making the multi-quark state a hadronic molecule, or into diquark anti-diquark substructures generating compact states. The $X(3872)$ state, also known as $\chi_{c1}(3872)$ [10], offers an ideal laboratory for addressing these questions.

The $X(3872)$ was observed by the Belle Collaboration [11] in $e^+e^- \rightarrow J/\psi\pi^+\pi^-$ and confirmed in many reactions and various final states [12–20]. Its quantum numbers are $J^{PC} = 1^{++}$ [15]. The most salient feature of this state is that its mass is very close to the $D^0\bar{D}^{*0}$ threshold—the mass measured from a Flatté analysis by the LHCb Collaboration is $M_X = 3871.69^{+0.00+0.05}_{-0.04-0.13}$ MeV [21], while the $D^0\bar{D}^{*0}$ threshold is at (3871.69 ± 0.07) MeV [10]. Despite the extremely small phase space, the $X(3872)$ was found to decay into $D^0\bar{D}^{*0}$ and $D^0\bar{D}^0\pi^0$ with large branching fractions [22–24]. These features suggest that this state be a hadronic molecule [25–30] (see Ref. [31] for a review). However, there are other interpretations. For instance, the

$X(3872)$ was explained as a compact tetraquark state in Ref. [32]. Because the quark-gluon interactions are isospin-independent, one distinct prediction in such a tetraquark model is the existence of an isospin triplet as flavor partners of the $X(3872)$. The charged partner of the $X(3872)$ was searched for by Belle in the $J/\psi\pi^+\pi^0$ invariant mass distributions from B meson decays [33], but no evidence was found.

In this Letter, based on chiral effective field theory (EFT) with the $X(3872)$ properties as input, we will show in a model-independent way that the $X(3872)$ should have isovector partners also if it is a $D\bar{D}^*$ hadronic molecule. They are virtual states of the scattering matrix, and their signals as either a mild cusp or dip at the $D\bar{D}^*$ threshold should be weak. It should be noted that virtual states can only appear for hadronic molecular states [34]. Thus a confirmation of our claim would at the same time be a proof for the molecular nature of the $X(3872)$ as well as its spin partners.

Symmetry analysis.—At energies very close to the $D\bar{D}^*$ thresholds, we can focus on S -wave meson-meson scattering and neglect higher partial waves. Let us first analyze consequences of heavy quark spin symmetry [35]. In the heavy quark limit, heavy quark spin decouples and the total angular momentum of the light degrees of freedom j_ℓ becomes a good quantum number. The D and D^* mesons are organized into doublets with $j_\ell^P = 1/2^-$, denoted as H . In addition they can be grouped into isospin doublets, e.g. $D = (D^+, D^0)^T$. Thus, the S -wave states

containing $H\bar{H}$ pairs can be arranged to form a definite isospin, I , and j_ℓ . In particular, they can be decomposed into four families [3, 36], two ($I = 0, 1$) with $j_\ell = 0$:

$$0_{\ell I}^{--} \otimes 0_{c\bar{c}}^{++} = 0_I^{++}, \quad 0_{\ell I}^{--} \otimes 1_{c\bar{c}}^{--} = 1_I^{+-}, \quad (1)$$

and the other two ($I = 0, 1$) with $j_\ell = 1$:

$$1_{\ell I}^{--} \otimes 0_{c\bar{c}}^{++} = 1_I^{+-}, \quad 1_{\ell I}^{--} \otimes 1_{c\bar{c}}^{--} = 0_I^{++} \oplus 1_I^{++} \oplus 2_I^{++}. \quad (2)$$

Here, the light quark-antiquark pair couples to the charm quark-antiquark pair, $j_{\ell I}^{PC} \otimes s_{c\bar{c}}^{PC}$, to form the $H\bar{H}$ pairs with quantum numbers J_I^{PC} . Furthermore, P and C denote the parity and charge parity, respectively, and J denotes the total angular momentum of $H\bar{H}$. Therefore, for the $X(3872)$ being a $J_I^{PC} = 1_0^{++}$ hadronic molecular state, one can predict the existence of three additional isoscalar states with 0_0^{++} , 1_0^{+-} , and 2_0^{++} , respectively, in the strict heavy quark limit [37, 38]. In Eq. (2), the $J_I^{PC} = 0_I^{++}$ and 1_I^{+-} states are mixtures of different charmed meson pairs [39], namely,

$$\begin{aligned} J_I^{PC} = 0_I^{++} : & \quad \frac{\sqrt{3}}{2} |D\bar{D}\rangle_I - \frac{1}{2} |D^*\bar{D}^*\rangle_I, \\ J_I^{PC} = 1_I^{+-} : & \quad \frac{1}{\sqrt{2}} \left[|(D\bar{D}^*)^{[C=-]}\rangle_I + |D^*\bar{D}^*\rangle_I \right], \end{aligned} \quad (3)$$

respectively, with $(D\bar{D}^*)^{[C=-]}$ the negative C -parity normalized combination of $D\bar{D}^*$ and $\bar{D}D^*$. The $J_I^{PC} = 1_I^{++}$ and 2_I^{++} states are purely $D\bar{D}^*$ and $D^*\bar{D}^*$, respectively. In particular, a $D^*\bar{D}^*$ molecule with 2_0^{++} is generally expected [36, 38, 40–42], using as input only the $X(3872)$ mass.

One more piece of information that can be used to constrain the $H\bar{H}$ molecule is the ratio of the branching fractions of the $X(3872)$ decays into $J/\psi\rho^0$ and $J/\psi\omega$, which is from isospin breaking and thus constrains the $I(j_\ell) = 1(1)$ sector [40, 43–47]. The ratio of branching fractions can be used to extract the ratio of the decay amplitudes of the $X(3872)$ decays into $J/\psi\rho^0$ and $J/\psi\omega$ [48, 49]. The most recent determination by the LHCb Collaboration is [50]

$$R_X = \left| \frac{\mathcal{M}_{X(3872) \rightarrow J/\psi\rho^0}}{\mathcal{M}_{X(3872) \rightarrow J/\psi\omega}} \right| = 0.29 \pm 0.04. \quad (4)$$

The $X(3872)$ flavor space wave function as a molecular state is given by

$$|X\rangle = \frac{1}{\sqrt{2}} \left(|(D\bar{D}^*)_0^{[C=+]}\rangle + |(D\bar{D}^*)_{\pm}^{[C=+]}\rangle \right), \quad (5)$$

where the first and second term in the parentheses are the positive C -parity pairs of the neutral $(D^0\bar{D}^{*0} - \bar{D}^0D^{*0})/\sqrt{2}$ and charged $(D^+D^{*-} - D^-D^{*+})/\sqrt{2}$ mesons, respectively. Being a physical observable, the ratio in Eq. (4) is scale-independent, and is related to the the couplings of the

$X(3872)$ to the charged and neutral $D\bar{D}^*$ pairs, $g_{X\pm}$ and g_{X0} , respectively, as

$$R_X = \left| \frac{1 - R_{\pm/0}}{1 + R_{\pm/0}} \right|, \quad R_{\pm/0} \equiv \frac{g_{X\pm}}{g_{X0}}. \quad (6)$$

Here, we have factorized the X decay amplitudes into a long-distance and a short-distance part [51], with the long-distance part given by the couplings to the charmed meson pairs,

$$\mathcal{M}_{[X \rightarrow J/\psi V]} = \frac{1}{\sqrt{2}} (g_{X0} \pm g_{X\pm}) \mathcal{M}_{[D\bar{D}^* \rightarrow J/\psi V]}^{\text{s.d.}}, \quad (7)$$

where $V = \rho^0$ or ω and the sign is “−” (“+”) for ρ^0 (ω). Since the short distance $D\bar{D}^* \rightarrow J/\psi V$ amplitudes should be the same up to small flavor SU(3)-breaking corrections, the short-distance part cancels out for the two decays. An equivalent relation has been derived in Refs. [45, 46]. Using Eq. (4), one obtains

$$R_{\pm/0} = 0.55 \pm 0.05, \quad (8)$$

which is sizably different from the value obtained in Refs. [37, 42, 44], where the ratio in Eq. (4) was assumed to be sensitive to the cutoff-dependent wave function of the $X(3872)$ at the origin. Since the squared couplings $g_{X\pm}^2$ and g_{X0}^2 correspond to the residues of the $X(3872)$ pole in the elastic scattering amplitudes of the charged and neutral meson pairs, respectively, the ratio $R_{\pm/0}$ and the $X(3872)$ mass as two inputs can be employed to constrain the $j_\ell = 1$ S -wave $H\bar{H}$ interactions in both the isoscalar and isovector channels.

Predictions.—Similar to the matured chiral EFT for nucleon-nucleon interaction [52], one can formulate a chiral EFT for the $D\bar{D}^*$ systems. The $D\bar{D}^*$ interactions can be described as a sum of contact terms and one-pion exchange (OPE) derived from the $D^*\pi$ chiral Lagrangian [53].

Because the $X(3872)$ is close to the $D^0\bar{D}^{*0}$ threshold, the contact terms can be expanded in powers of a small parameter Q/Λ , where Λ is a hard scale, and Q is the momentum scale of the charmed meson, which may be estimated as $\sqrt{2\mu_{\pm}\Delta} \simeq 126$ MeV, with μ_{\pm} the D^+D^{*-} reduced mass and $\Delta \equiv M_{D^{\pm}} + M_{D^{*\pm}} - M_{D^0} - M_{D^{*0}} = (8.23 \pm 0.07)$ MeV [10].

At leading order (LO), there are two low-energy constants (LECs), C_{0X} and C_{1X} , in the isoscalar and isovector channels, respectively [40].

$$V_{\text{ct}} = \frac{1}{2} \begin{pmatrix} C_{0X} + C_{1X} & C_{0X} - C_{1X} \\ C_{0X} - C_{1X} & C_{0X} + C_{1X} \end{pmatrix}, \quad (9)$$

where the matrix is in the channel space with the first and second channels being the neutral and charged $D\bar{D}^*$ pairs, respectively, specified in Eq. (5).

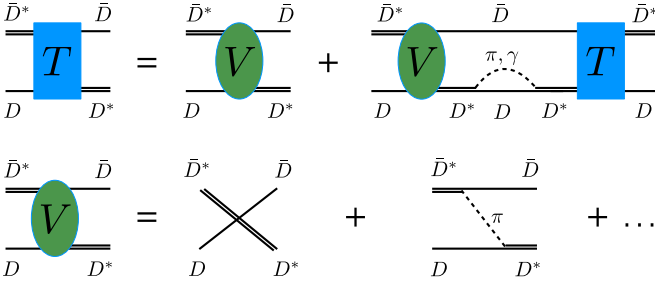


FIG. 1. $D\bar{D}^*$ scattering amplitudes with the full $D\bar{D}\pi$ three-body effects.

The amplitudes with the full $D\bar{D}\pi$ three-body effects are solutions of the Lippmann-Schwinger equation (LSE), as shown in Fig. 1,

$$T(E; p', p) = V(E; p', p) + \int \frac{l^2 dl}{2\pi^2} V(E; p', l) G(E; l) T(E; l, p), \quad (10)$$

with $E \equiv \sqrt{s} - M_{D^0} - M_{D^{*0}}$, \sqrt{s} the total energy in the center-of-mass (c.m.) frame, $p^{(l)}$ the magnitude of the initial (final) state c.m. three-momentum, G the Green's function for the two heavy mesons, and V the scattering potential including both the contact term and the OPE,

$$V(E; p', p) = V_{\text{ct}} + V_{\pi}(E; p', p). \quad (11)$$

The D^* widths are considered in G with both the $D\pi$ and $D\gamma$ contributions included. We treat the pions dynamically, approximate the photon loops in Fig. 1 by imaginary constants determined from the D^* radiative decay widths, and neglect the photon exchange potential, which binds the X atom as a $D^\pm D^{*\mp}$ Coulombic bound state [54] but does not affect the formation of hadronic molecular systems. Explicit expressions for the Green's function, the OPE potential, and technicalities regarding the choice of the integration path [55] can be found in the Supplemental Material [56].

The LSE is regularized with a momentum cutoff Λ and solved numerically [55, 57–60]. By requiring the real part of the $X(3872)$ pole to be $E = -\mathcal{B}_X$, where the binding energy is defined as $\mathcal{B}_X \equiv M_{D^0} + M_{D^{*0}} - M_{X(3872)}$, and

$$R_{\pm/0} = \lim_{E \rightarrow -\mathcal{B}_X - i\Gamma_{X0}/2} \frac{T_{21}(E)}{T_{11}(E)}, \quad (12)$$

with Γ_{X0} the open-charm partial width of $X(3872)$ from the $D\bar{D}\pi$ and $D\bar{D}\gamma$ modes through the D^* and \bar{D}^* decays, we can determine C_{0X} and C_{1X} . The solution was found employing an iterative procedure: We use the D^{*0} width 55.3 keV [61] as the initial value for Γ_{X0} , then C_{0X} and C_{1X} are fixed to reproduce both the real part of the $X(3872)$ pole and the coupling ratio in Eq. (8). From those LECs Γ_{X0} is recalculated, and the procedure is repeated until convergence is achieved. The resulting Γ_{X0}

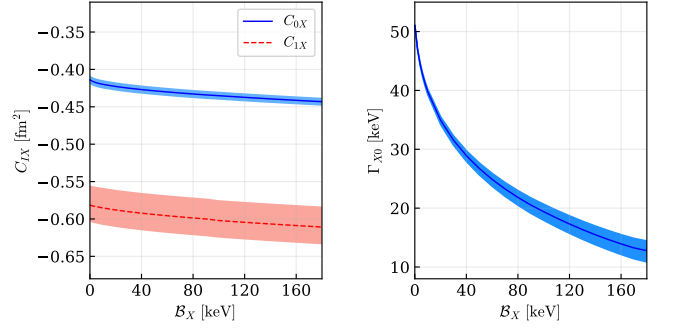


FIG. 2. Left: C_{0X} and C_{1X} at $\Lambda = 0.6$ GeV as functions of \mathcal{B}_X . Right: open-charm partial width of $X(3872)$ from the $D\bar{D}\pi$ and $D\bar{D}\gamma$ modes through D^* and \bar{D}^* decays. The bands are due to the uncertainty in Eq. (8).

is shown in the right panel of Fig. 2, and the LECs fixed in this way in the left panel for $\Lambda = 0.6$ GeV.

Similar to the case of the pionfull EFT treatment of the $T_{cc}(3875)$ in Ref. [59], the smallness of the expansion parameter Q/Λ ensures that the momentum independent contact terms can absorb the LO cutoff dependence, with the remainder a higher order effect relatively suppressed by $\mathcal{O}(Q^2/\Lambda^2)$. We have checked that varying the cutoff from 0.5 to 1.0 GeV, the predicted pole positions for the spin partner states (relative to the corresponding thresholds) change less than 5%.

Since all the S -wave $H\bar{H}$ meson interactions for pairs listed in Eq. (2) depend on the same C_{1X} , we can predict in a model-independent way the existence of isovector $H\bar{H}$ hadronic molecules using the C_{1X} value given in Fig. 2.¹ In particular, we can robustly predict the $J_I^{PC} = 1_1^{++}$ (W_{c1}) states as isovector $(D\bar{D}^*)^{[C=+]}$ hadronic molecules. With the notation in Eq. (5), the flavor wave function of the neutral W_{c1} is

$$|W_{c1}^0\rangle = \frac{1}{\sqrt{2}} \left(|(D\bar{D}^*)_0^{[C=+]}\rangle - |(D\bar{D}^*)_{\pm}^{[C=+]}\rangle \right). \quad (13)$$

Despite that the absolute value of C_{1X} is larger than that of C_{0X} at $\Lambda = 0.6$ GeV, the inclusion of the OPE leads to a weaker attraction in the isovector channel than the isoscalar one. Consequently, while the $X(3872)$ is a bound state pole in the stable D^* limit, the W_{c1}^0 is a virtual state pole of the same coupled-channel T -matrix in Eq. (10), located on the unphysical Riemann sheet of the complex E plane. Similarly, the charged W_{c1}^\pm is also a virtual state pole in the stable D^* limit, but of a single-channel T -matrix. In Fig. 3, we show the pole positions

¹ The predictions in Ref. [47] are cutoff dependent as the cutoff dependence in the $X \rightarrow J/\psi\rho$ and $J/\psi\omega$ amplitudes was not properly renormalized.

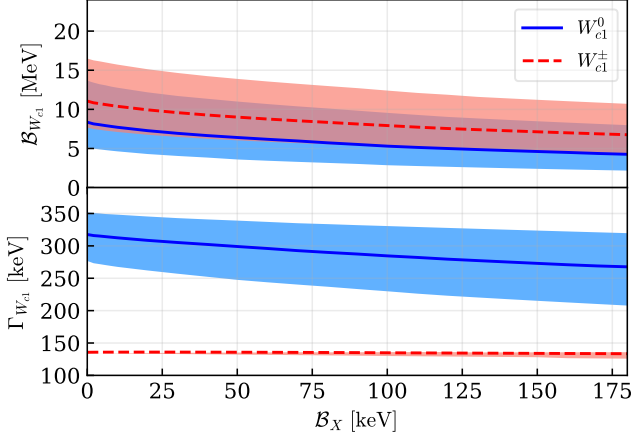


FIG. 3. Dependence of the predicted W_{c1} virtual state pole position on the input $X(3872)$ binding energy. The bands are from the uncertainty in Eq. (8). Upper: real part of the pole position with respect to the $D^0\bar{D}^{*0}$ (for W_{c1}^0) or D^0D^{*-} (for W_{c1}^\pm) threshold. Lower: twice the magnitude of the imaginary part of the W_{c1} pole position.

of the predicted W_{c1}^0 and W_{c1}^\pm virtual states, which are

$$\begin{aligned} W_{c1}^0 &: 3865.3_{-7.4}^{+4.2} - i0.15_{-0.03}^{+0.04} \text{ MeV}, \\ W_{c1}^\pm &: 3866.9_{-7.7}^{+4.6} - i(0.07 \pm 0.01) \text{ MeV}. \end{aligned} \quad (14)$$

The W_{c1} can decay into $J/\psi\pi\pi$ without breaking isospin symmetry, and the neutral one should decay into $J/\psi\pi^+\pi^-$, which is the discovery channel of the $X(3872)$ [11]. Thus, one natural question is why its signal and the signal of the charged W_{c1}^\pm states have not been observed [33]. To answer this question, we show the line shapes that emerge from the $(D\bar{D}^*)_0^{[C=+]}_-$ $(D\bar{D}^*)_0^{[C=+]}_+$ coupled-channel T matrix and the isovector $D^+\bar{D}^{*0}$ single-channel scattering amplitude in Fig. 4, where $B_X = 180$ keV is used as input for the $X(3872)$ binding energy. Being virtual states, the W_{c1} appear as threshold cusps. In the upper plot, the W_{c1}^0 signal is partly hidden under the $X(3872)$ signal which is represented by the huge narrow peak around the $D^0\bar{D}^{*0}$ threshold. The height of this peak depends crucially on the $X(3872)$ binding energy. For $B_X > 0$, the maximum is located at $-\mathcal{B}_X$. In that case, since the peak is below threshold, the maximal $|T_{ij}|$ values are larger than the values at the $D^0\bar{D}^{*0}$ threshold. It is also more than one order of magnitude larger than the cusps at the D^+D^{*-} threshold as well as the cusp in the $D^+\bar{D}^{*0}$ channel, explaining why so far no significant signal around 3880 MeV has been reported. Furthermore, subtracting out the $X(3872)$ contribution significantly reduces the peak at the lower threshold and modifies the structure at the higher. The line shape of $|T_{ij} - g_{Xi}g_{Xj}/(E + \mathcal{B}_X + i\Gamma_{X0}/2)|$, with g_{Xi} the coupling of $X(3872)$ to channel- i , is shown in the right panel of

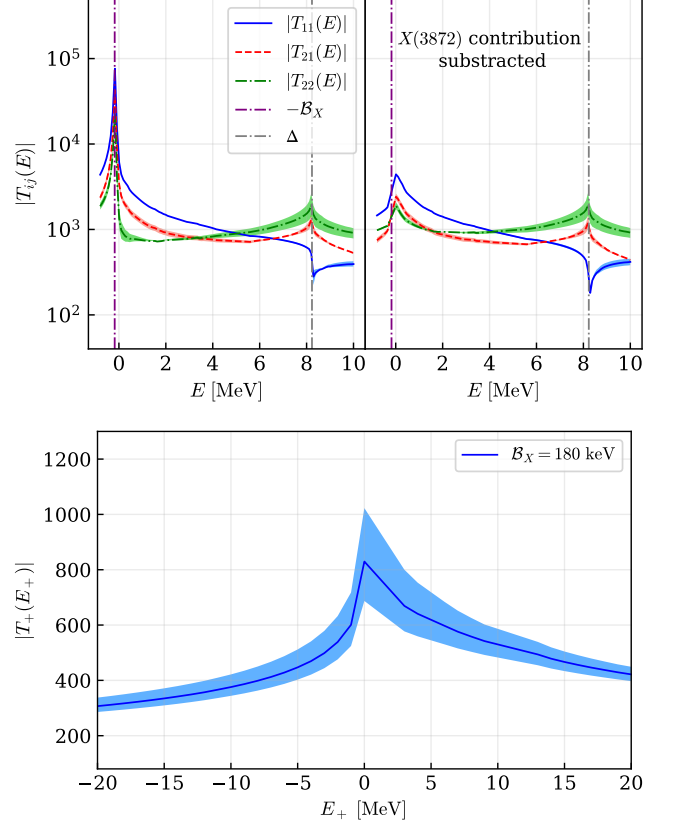


FIG. 4. Upper: Line shapes of the S -wave $D^0\bar{D}^{*0}$ - D^+D^{*-} scattering T -matrix elements, where the left and right parts are for the full T -matrix elements and the T -matrix elements with the $X(3872)$ pole contribution subtracted, respectively. Lower: Line shape of the single-channel $D^+\bar{D}^{*0}$ scattering T -matrix element, with E_+ defined relative to the $D^+\bar{D}^{*0}$ threshold. Here \mathcal{B}_X is set to 180 keV and the uncertainty is from Eq. (8).

the upper plot in Fig. 4. It is evident that the remaining line shapes possess threshold cusps of similar strengths at both the $D^0\bar{D}^{*0}$ and D^+D^{*-} thresholds.

The dip in the $|T_{11}(E)|$ line shape at the threshold of charged charmed meson pair is due to the strong S -wave attraction of the $(D\bar{D}^*)_0^{[C=+]}_-$ pair. It is another manifestation of the mechanism introduced in Ref. [62], which also offers a natural explanation [63] of the dip around the $X(3872)$ mass in e^+e^- direction production cross section measured by BESIII [64].

However, if the $X(3872)$ approaches the zero binding limit, that is $\mathcal{B}_X \rightarrow 0$, the residues of the T -matrix elements at the $X(3872)$ pole will be significantly reduced since they scale as $\sqrt{2\mu_0\mathcal{B}_X}$.² Then removing the $X(3872)$ pole contribution would hardly change the line shapes, and the W_{c1} signals would be relatively more

² No such relation exists for virtual states.

prominent, in conflict with experiment. Therefore, we conclude from the above analysis that the $X(3872)$ must be either a bound state with a non-vanishing binding energy or a very close to threshold virtual state in order to prevent a strong signal from the isovector W_{c1} states.

In the strict heavy quark limit, when D and D^* are degenerate, the W_{c1} should have isovector heavy quark spin partners with $J_I^{PC} = 0_1^{++}$, 2_1^{++} and 1_1^{+-} listed in Eq. (2). As shown in Eq. (3), the first one involves both S -wave $D\bar{D}$ and $D^*\bar{D}^*$, and the third one, which, mixing with the 1_1^{+-} state from Eq. (1), form the $Z_c(3900)$ [65, 66] and the $Z_c(4020)$ [67, 68], involves both S -wave $D\bar{D}^*$ and $D^*\bar{D}^*$. In addition, the second one can decay into $D\bar{D}$ and $D\bar{D}^*$ in D waves. Hence, a full calculation of all these cases would involve coupled channels with threshold differences of about 0.14 or 0.28 GeV, which relate to quite large momentum scales of the order of 0.5 and 0.7 GeV, respectively, requiring the inclusion of higher terms in the chiral expansion to reach sufficient accuracy. Moreover, a proper treatment of the then unavoidable D -wave contributions needs an S - D counterterm promoted to LO to render the results regulator independent [69, 70]. To fix this counterterm, additional data need to be included. Thus, we discuss these sectors more qualitatively in terms of a pionless theory. The LECs C_{0X} and C_{1X} are determined similarly as above. We checked that in the pionless theory the features of the results discussed above remain (for details, see the Supplemental Material [56]). For example, a virtual state pole is obtained for W_{c1} by about 10 MeV below threshold. Varying the two-meson reduced mass between $M_D/2$ and $M_{D^*}/2$, the virtual energy changes only by ± 3 MeV. Therefore, we anticipate virtual states in all the 0_1^{++} (W_{c0}), 1_1^{+-} (Z_c), and 2_1^{++} (W_{c2}) channels. Yet, since a coupling to higher channels effectively provides an additional attraction, the first two virtual states could be closer to threshold or even become bound state(s).

Summary.—In this Letter, we show that the $X(3872)$ treated as an isoscalar $D\bar{D}^*$ hadronic molecule, must have an isovector partner with the same particle content and $J_I^{PC} = 1_1^{++}$, based on chiral EFT employing only $X(3872)$ properties as input. The predicted states are virtual states in the scattering matrix that leave an imprint in the data either as a mild cusp or dip at the $D\bar{D}^*$ threshold. The pole positions are at $3865.3_{-7.4}^{+4.2} - i0.15_{-0.03}^{+0.04}$ MeV for W_{c1}^0 and $3866.9_{-7.7}^{+4.6} - i(0.07 \pm 0.01)$ MeV for W_{c1}^\pm . Moreover, the states should have isovector heavy quark spin partners with $J_I^{PC} = 2_1^{++}$ (W_{c2}), 1_1^{+-} (corresponding to a mixture of $Z_c(3900)$ and $Z_c(4020)$), and 0_1^{++} (W_{c0}). All these are expected to be virtual states, though channel couplings to $D^*\bar{D}^*$ in some cases may promote a virtual state to a bound one. While isovector partner states are expected also for compact tetraquarks [32], only a molecular nature allows for virtual states [34]. Virtual states leave an imprint in the data exactly at threshold which is thus a model-

independent prediction from the molecular scenario discussed in this Letter.

The findings here imply that the resonant peak in the $J/\psi\pi^+\pi^-$ distributions around 3872 MeV is not purely from the $X(3872)$ but also contains contributions from the W_{c1}^0 state. The charged W_{c1}^\pm state should have a threshold cusp in the D^+D^{*-} invariant mass distribution, and can be searched for in high-statistics data samples of the $J/\psi\pi^\pm\pi^0$. The charged W_{c0}^\pm and W_{c2}^\pm , whose mass predictions are more uncertain, may also be searched for in the same final state.

We are grateful to Alexey Nefediev and Bing-Song Zou for useful discussions. ZHZ would like to thank Zhao-Sai Jia for checking the numerical results. This work is supported in part by the National Key R&D Program of China under Grant No. 2023YFA1606703; by the Chinese Academy of Sciences (CAS) under Grants No. YSBR-101 and No. XDB34030000; by the National Natural Science Foundation of China (NSFC) under Grants No. 12125507, No. 12361141819, and No. 12047503; and by NSFC and the Deutsche Forschungsgemeinschaft (DFG) through the funds provided to the Sino-German Collaborative Research Center CRC110 “Symmetries and the Emergence of Structure in QCD” (DFG Project-ID 196253076). A.R., in addition, thanks the CAS President’s International Fellowship Initiative (PIFI) (Grant No. 2024VMB0001) for partial financial support.

* zhangzhenhua@itp.ac.cn
 † teng@hiskp.uni-bonn.de
 ‡ xiangkun@hiskp.uni-bonn.de
 § fkguo@itp.ac.cn

- [1] A. Hosaka, T. Iijima, K. Miyabayashi, Y. Sakai, and S. Yasui, Exotic hadrons with heavy flavors: X, Y, Z, and related states, *PTEP* **2016**, 062C01 (2016), [arxiv:1603.09229 \[hep-ph\]](#).
- [2] A. Esposito, A. Pilloni, and A. D. Polosa, Multiquark resonances, *Phys. Rept.* **668**, 1 (2017), [arxiv:1611.07920 \[hep-ph\]](#).
- [3] F.-K. Guo, C. Hanhart, U.-G. Meißner, Q. Wang, Q. Zhao, and B.-S. Zou, Hadronic molecules, *Rev. Mod. Phys.* **90**, 015004 (2018), [arxiv:1705.00141 \[hep-ph\]](#).
- [4] S. L. Olsen, T. Skwarnicki, and D. Zieminska, Nonstandard heavy mesons and baryons: Experimental evidence, *Rev. Mod. Phys.* **90**, 015003 (2018), [arxiv:1708.04012 \[hep-ph\]](#).
- [5] M. Karliner, J. L. Rosner, and T. Skwarnicki, Multiquark states, *Ann. Rev. Nucl. Part. Sci.* **68**, 17 (2018), [arxiv:1711.10626 \[hep-ph\]](#).
- [6] N. Brambilla, S. Eidelman, C. Hanhart, A. Nefediev, C.-P. Shen, C. E. Thomas, A. Vairo, and C.-Z. Yuan, The XYZ states: Experimental and theoretical status and perspectives, *Phys. Rept.* **873**, 1 (2020), [arxiv:1907.07583 \[hep-ex\]](#).
- [7] G. Yang, J. Ping, and J. Segovia, Tetra- and penta-quark

- structures in the constituent quark model, *Symmetry* **12**, 1869 (2020), [arxiv:2009.00238 \[hep-ph\]](#).
- [8] H.-X. Chen, W. Chen, X. Liu, Y.-R. Liu, and S.-L. Zhu, An updated review of the new hadron states, *Rept. Prog. Phys.* **86**, 026201 (2022), [arxiv:2204.02649 \[hep-ph\]](#).
- [9] L. Meng, B. Wang, G.-J. Wang, and S.-L. Zhu, Chiral perturbation theory for heavy hadrons and chiral effective field theory for heavy hadronic molecules, *Phys. Rept.* **1019**, 2266 (2023), [arxiv:2204.08716 \[hep-ph\]](#).
- [10] R. L. Workman *et al.* (Particle Data Group), Review of Particle Physics, *PTEP* **2022**, 083C01 (2022).
- [11] S. K. Choi *et al.* (Belle), Observation of a narrow charmonium-like state in exclusive $B^\pm \rightarrow K^\pm \pi^+ \pi^- J/\psi$ decays, *Phys. Rev. Lett.* **91**, 262001 (2003), [arxiv:hep-ex/0309032](#).
- [12] V. M. Abazov *et al.* (D0), Observation and properties of the $X(3872)$ decaying to $J/\psi \pi^+ \pi^-$ in $p\bar{p}$ collisions at $\sqrt{s} = 1.96$ TeV, *Phys. Rev. Lett.* **93**, 162002 (2004), [arXiv:hep-ex/0405004](#).
- [13] G. Gokhroo *et al.* (Belle), Observation of a near-threshold $D^0 \bar{D}^0 \pi^0$ enhancement in $B \rightarrow D^0 \bar{D}^0 \pi^0 K$ decay, *Phys. Rev. Lett.* **97**, 162002 (2006), [arxiv:hep-ex/0606055](#).
- [14] P. del Amo Sanchez *et al.* (BaBar), Evidence for the decay $X(3872) \rightarrow J/\psi \omega$, *Phys. Rev. D* **82**, 011101 (2010), [arxiv:1005.5190 \[hep-ex\]](#).
- [15] R. Aaij *et al.* (LHCb), Determination of the $X(3872)$ meson quantum numbers, *Phys. Rev. Lett.* **110**, 222001 (2013), [arxiv:1302.6269 \[hep-ex\]](#).
- [16] M. Ablikim *et al.* (BESIII), Observation of $e^+ e^- \rightarrow \gamma X(3872)$ at BESIII, *Phys. Rev. Lett.* **112**, 092001 (2014), [arxiv:1310.4101 \[hep-ex\]](#).
- [17] M. Aaboud *et al.* (ATLAS), Measurements of $\psi(2S)$ and $X(3872) \rightarrow J/\psi \pi^+ \pi^-$ production in pp collisions at $s = 8$ TeV with the ATLAS detector, *JHEP* **01** (CERN-EP-2016-193), 117, [arxiv:1610.09303 \[hep-ex\]](#).
- [18] M. Ablikim *et al.* (BESIII), Observation of the decay $X(3872) \rightarrow \pi^0 \chi_{c1}(1P)$, *Phys. Rev. Lett.* **122**, 202001 (2019), [arxiv:1901.03992 \[hep-ex\]](#).
- [19] A. M. Sirunyan *et al.* (CMS), Evidence for $X(3872)$ in Pb-Pb Collisions and Studies of its Prompt Production at $\sqrt{s_{NN}} = 5.02$ TeV, *Phys. Rev. Lett.* **128**, 032001 (2022), [arXiv:2102.13048 \[hep-ex\]](#).
- [20] M. Ablikim *et al.* (BESIII), Observation of a new $X(3872)$ production process $e^+ e^- \rightarrow \omega X(3872)$, *Phys. Rev. Lett.* **130**, 151904 (2023), [arxiv:2212.07291 \[hep-ex\]](#).
- [21] R. Aaij *et al.* (LHCb), Study of the lineshape of the $\chi_{c1}(3872)$ state, *Phys. Rev. D* **102**, 092005 (2020), [arxiv:2005.13419 \[hep-ex\]](#).
- [22] T. Aushev *et al.* (Belle), Study of the $B \rightarrow X(3872)(\rightarrow D^{*0} \bar{D}^0) K$ decay, *Phys. Rev. D* **81**, 031103 (2010), [arxiv:0810.0358 \[hep-ex\]](#).
- [23] C. Li and C.-Z. Yuan, Determination of the absolute branching fractions of $X(3872)$ decays, *Phys. Rev. D* **100**, 094003 (2019), [arxiv:1907.09149 \[hep-ex\]](#).
- [24] E. Braaten, L.-P. He, and K. Inles, Branching Fractions of the $X(3872)$, [arXiv:1908.02807 \[hep-ph\]](#) (2019), [arxiv:1908.02807 \[hep-ph\]](#).
- [25] F. E. Close and P. R. Page, The $D^{*0} \bar{D}^0$ threshold resonance, *Phys. Lett. B* **578**, 119 (2004), [arxiv:hep-ph/0309253](#).
- [26] S. Pakvasa and M. Suzuki, On the hidden charm state at 3872 MeV, *Phys. Lett. B* **579**, 67 (2004), [arxiv:hep-ph/0309294](#).
- [27] M. Voloshin, Interference and binding effects in decays of possible molecular component of $X(3872)$, *Phys. Lett. B* **579**, 316 (2004), [arxiv:hep-ph/0309307](#).
- [28] E. S. Swanson, Short range structure in the $X(3872)$, *Phys. Lett. B* **588**, 189 (2004), [arxiv:hep-ph/0311229](#).
- [29] E. Braaten and M. Kusunoki, Low-energy universality and the new charmonium resonance at 3870 MeV, *Phys. Rev. D* **69**, 074005 (2004), [arxiv:hep-ph/0311147](#).
- [30] N. A. Törnqvist, Isospin breaking of the narrow charmonium state of Belle at 3872 MeV as a deuson, *Phys. Lett. B* **590**, 209 (2004), [arxiv:hep-ph/0402237](#).
- [31] Y. S. Kalashnikova and A. V. Nefediev, $X(3872)$ in the molecular model, *Phys. Usp.* **62**, 568 (2019), [arxiv:1811.01324 \[hep-ph\]](#).
- [32] L. Maiani, F. Piccinini, A. D. Polosa, and V. Riquer, Diquark-antidiquarks with hidden or open charm and the nature of $X(3872)$, *Phys. Rev. D* **71**, 014028 (2005), [arxiv:hep-ph/0412098](#).
- [33] S. K. Choi *et al.* (Belle), Bounds on the width, mass difference and other properties of $X(3872) \rightarrow \pi^+ \pi^- J/\psi$ decays, *Phys. Rev. D* **84**, 052004 (2011), [arxiv:1107.0163 \[hep-ex\]](#).
- [34] I. Matuschek, V. Baru, F.-K. Guo, and C. Hanhart, On the nature of near-threshold bound and virtual states, *Eur. Phys. J. A* **57**, 101 (2021), [arXiv:2007.05329 \[hep-ph\]](#).
- [35] N. Isgur and M. B. Wise, Weak decays of heavy mesons in the static quark approximation, *Phys. Lett. B* **232**, 113 (1989).
- [36] J. Nieves and M. P. Valderrama, The Heavy Quark Spin Symmetry Partners of the $X(3872)$, *Phys. Rev. D* **86**, 056004 (2012), [arxiv:1204.2790 \[hep-ph\]](#).
- [37] C. Hidalgo-Duque, J. Nieves, A. Ozpineci, and V. Zamiralov, $X(3872)$ and its Partners in the Heavy Quark Limit of QCD, *Phys. Lett. B* **727**, 432 (2013), [arxiv:1305.4487 \[hep-ph\]](#).
- [38] V. Baru, E. Epelbaum, A. A. Filin, C. Hanhart, U.-G. Meißner, and A. V. Nefediev, Heavy-quark spin symmetry partners of the $X(3872)$ revisited, *Phys. Lett. B* **763**, 20 (2016), [arxiv:1605.09649 \[hep-ph\]](#).
- [39] T.-R. Hu, S. Chen, and F.-K. Guo, Entanglement suppression and low-energy scattering of heavy mesons, (2024), [arxiv:2404.05958 \[hep-ph\]](#).
- [40] C. Hidalgo-Duque, J. Nieves, and M. P. Valderrama, Light flavor and heavy quark spin symmetry in heavy meson molecules, *Phys. Rev. D* **87**, 076006 (2013), [arxiv:1210.5431 \[hep-ph\]](#).
- [41] F.-K. Guo, C. Hidalgo-Duque, J. Nieves, and M. P. Valderrama, Consequences of heavy quark symmetries for hadronic molecules, *Phys. Rev. D* **88**, 054007 (2013), [arxiv:1303.6608 \[hep-ph\]](#).
- [42] M. Albaladejo, F.-K. Guo, C. Hidalgo-Duque, J. Nieves, and M. P. Valderrama, Decay widths of the spin-2 partners of the $X(3872)$, *Eur. Phys. J. C* **75**, 547 (2015), [arxiv:1504.00861 \[hep-ph\]](#).
- [43] D. Gamermann and E. Oset, Isospin breaking effects in the $X(3872)$ resonance, *Phys. Rev. D* **80**, 014003 (2009), [arxiv:0905.0402 \[hep-ph\]](#).
- [44] D. Gamermann, J. Nieves, E. Oset, and E. R. Arriola, Couplings in coupled channels versus wave functions: Application to the $X(3872)$ resonance, *Phys. Rev. D* **81**, 014029 (2010).
- [45] N. Li and S.-L. Zhu, Isospin breaking, coupled-channel effects, and $X(3872)$, *Phys. Rev. D* **86**, 074022 (2012),

- arxiv:1207.3954 [hep-ph].
- [46] L. Meng, G.-J. Wang, B. Wang, and S.-L. Zhu, Revisit the isospin violating decays of $X(3872)$, *Phys. Rev. D* **104**, 094003 (2021), arxiv:2109.01333 [hep-ph].
 - [47] T. Ji, X.-K. Dong, M. Albaladejo, M.-L. Du, F.-K. Guo, and J. Nieves, Establishing the heavy quark spin and light flavor molecular multiplets of the $X(3872)$, $Z_c(3900)$ and $X(3960)$, *Phys. Rev. D* **106**, 094002 (2022), arxiv:2207.08563 [hep-ph].
 - [48] M. Suzuki, $X(3872)$ boson: Molecule or charmonium, *Phys. Rev. D* **72**, 114013 (2005), arxiv:hep-ph/0508258.
 - [49] C. Hanhart, Yu. S. Kalashnikova, A. E. Kudryavtsev, and A. V. Nefediev, Remarks on the quantum numbers of $X(3872)$ from the invariant mass distributions of the $\rho J/\psi$ and $\omega J/\psi$ final states, *Phys. Rev. D* **85**, 011501 (2012), arxiv:1111.6241 [hep-ph].
 - [50] R. Aaij and others (LHCb), Observation of sizeable ω contribution to $\chi_{c1}(3872) \rightarrow \pi^+ \pi^- J/\psi$ decays, *Phys. Rev. D* **108**, L011103 (2023), arxiv:2204.12597 [hep-ex].
 - [51] E. Braaten and M. Kusunoki, Factorization in the production and decay of the $X(3872)$, *Phys. Rev. D* **72**, 014012 (2005), arxiv:hep-ph/0506087.
 - [52] E. Epelbaum, H.-W. Hammer, and U.-G. Meißner, Modern theory of nuclear forces, *Rev. Mod. Phys.* **81**, 1773 (2009), arxiv:0811.1338 [nucl-th].
 - [53] M. B. Wise, Chiral perturbation theory for hadrons containing a heavy quark, *Phys. Rev. D* **45**, R2188 (1992).
 - [54] Z.-H. Zhang and F.-K. Guo, $D^\pm D^{*\mp}$ Hadronic Atom as a Key to Revealing the $X(3872)$ Mystery, *Phys. Rev. Lett.* **127**, 012002 (2021), arxiv:2012.08281 [hep-ph].
 - [55] X.-K. Dong, T. Ji, F.-K. Guo, U.-G. Meißner, and B.-S. Zou, Hints of the $J^{PC} = 0^{--}$ and 1^{--} $K^* \bar{K}_1(1270)$ molecules in the $J/\psi \rightarrow \phi \eta \eta'$ decay, arxiv:2402.02903 [hep-ph] (2024), arxiv:2402.02903 [hep-ph].
 - [56] See Supplemental Material for explicit expressions for details of the LSE and results in the pionless theory.
 - [57] M. Döring, C. Hanhart, F. Huang, S. Krewald, and U.-G. Meissner, Analytic properties of the scattering amplitude and resonances parameters in a meson exchange model, *Nucl. Phys. A* **829**, 170 (2009), arxiv:0903.4337 [nucl-th].
 - [58] V. Baru, A. A. Filin, C. Hanhart, Yu. S. Kalashnikova, A. E. Kudryavtsev, and A. V. Nefediev, Three-body $D\bar{D}\pi$ dynamics for the $X(3872)$, *Phys. Rev. D* **84**, 074029 (2011), arxiv:1108.5644 [hep-ph].
 - [59] M.-L. Du, V. Baru, X.-K. Dong, A. Filin, F.-K. Guo, C. Hanhart, A. Nefediev, J. Nieves, and Q. Wang, Coupled-channel approach to T_{cc}^+ including three-body effects, *Phys. Rev. D* **105**, 014024 (2022), arxiv:2110.13765 [hep-ph].
 - [60] T. Ji, X.-K. Dong, F.-K. Guo, and B.-S. Zou, Prediction of a Narrow Exotic Hadronic State with Quantum Numbers $J^{PC} = 0^{--}$, *Phys. Rev. Lett.* **129**, 102002 (2022), arxiv:2205.10994 [hep-ph].
 - [61] F.-K. Guo, Novel Method for Precisely Measuring the $X(3872)$ Mass, *Phys. Rev. Lett.* **122**, 202002 (2019), arxiv:1902.11221 [hep-ph].
 - [62] X.-K. Dong, F.-K. Guo, and B.-S. Zou, Explaining the many threshold structures in the heavy-quark hadron spectrum, *Phys. Rev. Lett.* **126**, 152001 (2021), arxiv:2011.14517 [hep-ph].
 - [63] V. Baru *et al.*, How does the $X(3872)$ show up in e^+e^- collisions: dip versus peak, (2014), in preparation.
 - [64] M. Ablikim *et al.* (BESIII), Measurement of the $e^+e^- \rightarrow \pi^+ \pi^- J/\psi$ cross section in the vicinity of 3.872 GeV, *Phys. Rev. D* **107**, 032007 (2023), arxiv:2209.12007 [hep-ex].
 - [65] M. Ablikim *et al.* (BESIII), Observation of a Charged Charmoniumlike Structure in $e^+e^- \rightarrow \pi^+ \pi^- J/\psi$ at $\sqrt{s} = 4.26$ GeV, *Phys. Rev. Lett.* **110**, 252001 (2013), arxiv:1303.5949 [hep-ex].
 - [66] Z. Q. Liu *et al.* (Belle), Study of $e^+e^- \rightarrow \pi^+ \pi^- J/\psi$ and Observation of a Charged Charmoniumlike State at Belle, *Phys. Rev. Lett.* **110**, 252002 (2013), [Erratum: *Phys. Rev. Lett.* **111**, 019901 (2013)], arxiv:1304.0121 [hep-ex].
 - [67] M. Ablikim *et al.* (BESIII), Observation of a Charged Charmoniumlike Structure $Z_c(4020)$ and Search for the $Z_c(3900)$ in $e^+e^- \rightarrow \pi^+ \pi^- h_c$, *Phys. Rev. Lett.* **111**, 242001 (2013), arxiv:1309.1896 [hep-ex].
 - [68] M. Ablikim *et al.* (BESIII), Observation of a charged charmoniumlike structure in $e^+e^- \rightarrow (D^* \bar{D}^*)^\pm \pi^\mp$ at $\sqrt{s} = 4.26$ GeV, *Phys. Rev. Lett.* **112**, 132001 (2014), arxiv:1308.2760 [hep-ex].
 - [69] Q. Wang, V. Baru, A. A. Filin, C. Hanhart, A. V. Nefediev, and J. L. Wynen, Line shapes of the $Z_b(10610)$ and $Z_b(10650)$ in the elastic and inelastic channels revisited, *Phys. Rev. D* **98**, 074023 (2018), arxiv:1805.07453 [hep-ph].
 - [70] V. Baru, E. Epelbaum, A. A. Filin, C. Hanhart, A. V. Nefediev, and Q. Wang, Spin partners W_{bJ} from the line shapes of the $Z_b(10610)$ and $Z_b(10650)$, *Phys. Rev. D* **99**, 094013 (2019), arxiv:1901.10319 [hep-ph].

Supplemental Materials

Details of the Lippmann-Schwinger equation

The introduction of a dynamical pion in the interaction between $D\bar{D}^*$ leads to the emergence of nontrivial cuts in the $D\bar{D}^*$ scattering amplitude in two ways [55, 58–60]: first, the on-shellness of the exchanged pion between $D\bar{D}^*$, depicted in Fig. 5 (a); and second, the energy-dependent width of D^* , depicted in Fig. 5 (b). These two aspects are discussed in detail here.

The $D^*D\pi$ coupling can be described by the Lagrangian [53],

$$\mathcal{L}_{DD^*\pi} = -\frac{\sqrt{2}g}{F_\pi} \sqrt{m_D m_{D^*}} \{ [D(\partial^\mu \mathcal{P})D_\mu^{*\dagger} + D_\mu^*(\partial^\mu \mathcal{P})D^\dagger] - [\bar{D}(\partial^\mu \mathcal{P})^T \bar{D}_\mu^{*\dagger} + \bar{D}_\mu^*(\partial^\mu \mathcal{P})^T \bar{D}^\dagger] \}, \quad (15)$$

where $F_\pi = 92.1$ MeV is the pion decay constant, $g = 0.57$ is determined by the $D^* \rightarrow D\pi$ decay width [10], and

$$\begin{aligned} D &= (D^+, D^0), & \bar{D} &= (D^-, \bar{D}^0), \\ D^* &= (D^{*+}, D^{*0}), & \bar{D}^* &= (D^{*-}, \bar{D}^{*0}), \\ \mathcal{P} &= \begin{pmatrix} \pi^0/\sqrt{2} & \pi^+ \\ \pi^- & -\pi^0/\sqrt{2} \end{pmatrix}. \end{aligned} \quad (16)$$

We have used the following phase conventions for charge conjugation,

$$\hat{C}|D\rangle = |\bar{D}\rangle, \quad \hat{C}|D^*\rangle = -|\bar{D}^*\rangle. \quad (17)$$

OPE

Using the Lagrangian in Eq. (15), the OPE potential of the $D^0\bar{D}^{*0}-D^+D^{*-}$ coupled channels in S -wave can be expressed as

$$V_\pi(E; p', p) = \frac{g^2}{6F_\pi^2} \begin{pmatrix} \frac{1}{2}V_{D^0\pi^0\bar{D}^0}^{SS} & V_{D^0\pi^+D^-}^{SS} \\ V_{D^+\pi^-\bar{D}^0}^{SS} & \frac{1}{2}V_{D^+\pi^0D^-}^{SS} \end{pmatrix}, \quad (18)$$

with

$$V_{\alpha\beta\zeta}^{SS} = \frac{1}{2} \int_{-1}^1 dz \frac{q^2}{D_{\alpha\beta\zeta}^{\text{TOPT}}(E; p', p, z)}, \quad (19)$$

and $q^2 = p'^2 + p^2 - 2p'pz$. The propagator of the exchanged pion reads in time-ordered perturbation theory (TOPT) as

$$\frac{1}{D_{\alpha\beta\zeta}^{\text{TOPT}}} = \frac{1}{2E_\beta(q)} \left(\frac{1}{D_{\alpha\beta\zeta}^R} + \frac{1}{D_{\alpha^*\beta\zeta^*}^A} \right), \quad (20)$$

with

$$D_{\alpha\beta\zeta}^R = \sqrt{s} - E_\alpha(p) - E_\beta(q) - E_\zeta(p') + i\varepsilon, \quad (21)$$

$$D_{\alpha^*\beta\zeta^*}^A = \sqrt{s} - E_{\alpha^*}(p') - E_\beta(q) - E_{\zeta^*}(p) + i\varepsilon. \quad (22)$$

These two terms correspond to the diagrams in Fig. 5 (a) and (c), respectively. Here the energy for particle α with 3-momentum magnitude l is expressed as $E_\alpha(l) = \sqrt{l^2 + M_\alpha^2}$. The labels α^* and ζ^* represent D^* and \bar{D}^* , respectively, and their electric charges are given by

$$Q_e(\alpha^*) = Q_e(\alpha) + Q_e(\beta), \quad Q_e(\zeta^*) = Q_e(\beta) + Q_e(\zeta). \quad (23)$$

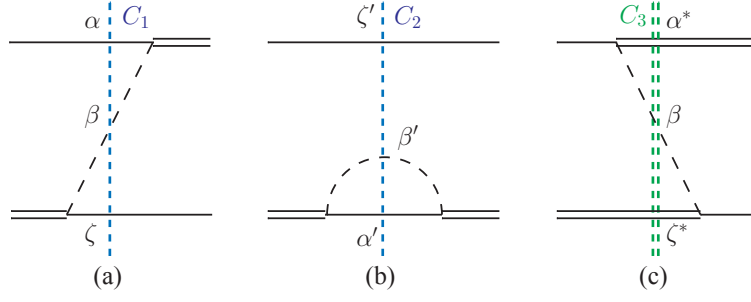


FIG. 5. Illustration of the 3-body cuts in the (a) retarded propagator, (b) D^* selfenergy, and (c) advanced propagator. The D^* , D , and π mesons are represented by the double solid, solid, and dashed lines, respectively. The three particles on the blue cut C_1 or C_2 can go on-shell in the physical region, while the three particles on the green cut C_3 cannot. The labels of the particles on the cuts are those in Eqs. (20) and (45).

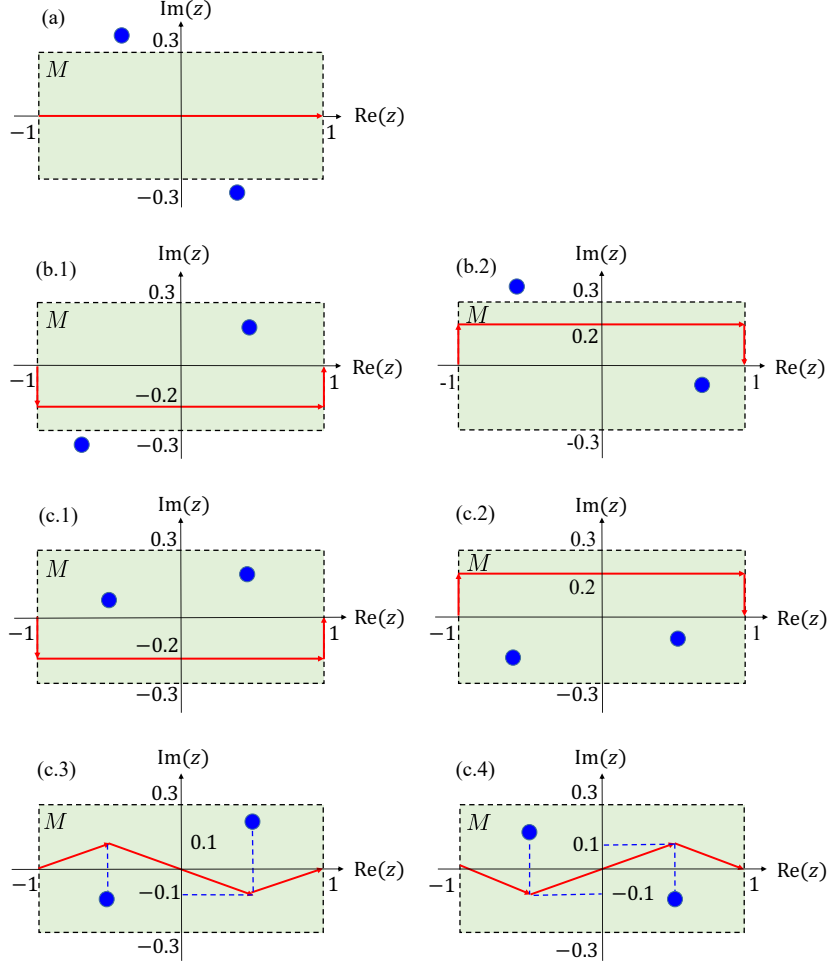


FIG. 6. Possible positions of the singularities z_{0R} and $z_{0\pi}$ (blue dots) relative to region M (shaded area) and the corresponding integration paths (in red).

The integrand of Eq. (19) is divergent at the roots z_{0R} and $z_{0\pi}$ of $D_{\alpha\beta\zeta}^R(E; p', p, z)$ and $E_\beta(q)$, respectively. One should deform the integration path to avoid the singularities being too close to it. We use the strategy in Ref. [55]. That is, we define a neighbourhood $M = \{z \in \mathbb{C} \mid -1 < \text{Re}[z] < 1, -0.3 < \text{Im}[z] < 0.3\}$ of $z \in [-1, 1]$ and choose the integration path properly according to the relative positions of z_{0R} and $z_{0\pi}$ to M . Without losing generality, we assume $\text{Re}[z_R] \geq \text{Re}[z_\pi]$ in the following discussion on the choice of the integration path. There are several cases:

- (a) $z_{0R} \notin M$ & $z_{0\pi} \notin M$. Both singularities are not in M . The integration path is just

$$C_a = \left\{ z \in \mathbb{R} \mid -1 \leq z \leq 1 \right\}, \quad (24)$$

like (a) in Fig. 6.

- (b) $(z_{0R} \in M \text{ \& } z_{0\pi} \notin M) \parallel (z_{0R} \notin M \text{ \& } z_{0\pi} \in M)$. Only one of the singularities is located in M and is denoted as z_M . The path depends on the position of z_M in M .

- (1) $\text{Im}[z_M] > 0$. The path is chosen as

$$C_{b1} = C_{b1}^{(1)} \cup C_{b1}^{(2)} \cup C_{b1}^{(3)}, \quad (25)$$

$$C_{b1}^{(1)} = \left\{ z(t) \in \mathbb{C} \mid z(t) = -1 - it/5, 0 \leq t \leq 1 \right\}, \quad (26)$$

$$C_{b1}^{(2)} = \left\{ z(t) \in \mathbb{C} \mid z(t) = -1 - i/5 + 2t, 0 \leq t \leq 1 \right\}, \quad (27)$$

$$C_{b1}^{(3)} = \left\{ z(t) \in \mathbb{C} \mid z(t) = 1 - i(1-t)/5, 0 \leq t \leq 1 \right\}, \quad (28)$$

like (b.1) in Fig. 6.

- (2) $\text{Im}[z_M] < 0$. The path is chosen as

$$C_{b2} = C_{b2}^{(1)} \cup C_{b2}^{(2)} \cup C_{b2}^{(3)}, \quad (29)$$

$$C_{b2}^{(1)} = \left\{ z(t) \in \mathbb{C} \mid z(t) = -1 + it/5, 0 \leq t \leq 1 \right\}, \quad (30)$$

$$C_{b2}^{(2)} = \left\{ z(t) \in \mathbb{C} \mid z(t) = -1 + i/5 + 2t, 0 \leq t \leq 1 \right\}, \quad (31)$$

$$C_{b2}^{(3)} = \left\{ z(t) \in \mathbb{C} \mid z(t) = 1 + i(1-t)/5, 0 \leq t \leq 1 \right\}, \quad (32)$$

like (b.2) in Fig. 6.

- (c) $z_{0R} \in M$ & $z_{0\pi} \in M$. Both singularities are in the region M . There are four cases of the singularity positions.

- (1) $\text{Im}[z_R] > 0$ & $\text{Im}[z_\pi] > 0$. Both singularities are on the upper half z plane. The path is chosen as $C_{c1} = C_{b1}$, like (c.1) in Fig. 6.
- (2) $\text{Im}[z_R] < 0$ & $\text{Im}[z_\pi] < 0$. Both singularities are on the lower half z plane. The path is chosen as $C_{c2} = C_{b2}$, like (c.2) in Fig. 6.
- (3) $\text{Im}[z_R] > 0$ & $\text{Im}[z_\pi] < 0$. The two singularities are on the opposite side of the real axis on the z plane, the integration path is chosen as

$$C_{c3} = C_{c3}^{(1)} \cup C_{c3}^{(2)} \cup C_{c3}^{(3)}, \quad (33)$$

$$C_{c3}^{(1)} = \left\{ z(t) \in \mathbb{C} \mid z(t) = -1 + (z_1 + 1)t, 0 \leq t \leq 1 \right\}, \quad (34)$$

$$C_{c3}^{(2)} = \left\{ z(t) \in \mathbb{C} \mid z(t) = z_1 + (z_2 - z_1)t, 0 \leq t \leq 1 \right\}, \quad (35)$$

$$C_{c3}^{(3)} = \left\{ z(t) \in \mathbb{C} \mid z(t) = z_2 + (1 - z_2)t, 0 \leq t \leq 1 \right\}, \quad (36)$$

like (c.3) in Fig. 6, where $z_1 = \text{Re}[z_{0\pi}] + i/10$, $z_2 = \text{Re}[z_{0R}] - i/10$.

- (4) $\text{Im}[z_R] < 0$ & $\text{Im}[z_\pi] > 0$. The two singularities are on opposite sides of the real axis on the z plane, and the integration path is chosen as

$$C_{c4} = C_{c4}^{(1)} \cup C_{c4}^{(2)} \cup C_{c4}^{(3)}, \quad (37)$$

$$C_{c4}^{(1)} = \left\{ z(t) \in \mathbb{C} \mid z(t) = -1 + (z_3 + 1)t, 0 \leq t \leq 1 \right\}, \quad (38)$$

$$C_{c4}^{(2)} = \left\{ z(t) \in \mathbb{C} \mid z(t) = z_3 + (z_4 - z_3)t, 0 \leq t \leq 1 \right\}, \quad (39)$$

$$C_{c4}^{(3)} = \left\{ z(t) \in \mathbb{C} \mid z(t) = z_4 + (1 - z_4)t, 0 \leq t \leq 1 \right\}, \quad (40)$$

like (c.4) in Fig. 6, where $z_3 = \text{Re}[z_{0\pi}] - i/10$, $z_4 = \text{Re}[z_{0R}] + i/10$.

D^* selfenergy

The Green's function in Eq.(10) is expressed as

$$G(E; l) = \begin{pmatrix} G_0(E; l) & 0 \\ 0 & G_{\pm}(E; l) \end{pmatrix} = \begin{pmatrix} \frac{1}{E - l^2/(2\mu_0) + i\Gamma_0^{\mathcal{D}}(E; l)/2} & 0 \\ 0 & \frac{1}{E - \Delta - l^2/(2\mu_{\pm}) + i2\Gamma_{\pm}^{\mathcal{D}}(E; l)/2} \end{pmatrix}, \quad (41)$$

with $\mu_0 = M_{D^0}M_{D^{*0}}/(M_{D^0} + M_{D^{*0}})$ and $\mu_{\pm} = M_{D^+}M_{D^{*-}}/(M_{D^+} + M_{D^{*-}})$. The energy-dependent decay widths of neutral and charged D^* mesons read

$$\begin{aligned} \Gamma_0^{\mathcal{D}}(E; l) &= \Gamma_{[D^{*0} \rightarrow D^0 \gamma]} + \frac{g^2 M_{D^+}}{12\pi F_{\pi}^2 M_{D^{*0}}} [\Sigma_{D^+ \pi^- D^0}(E; l, \mu_{\pm}) - \Sigma_{D^+ \pi^- D^0}(0; 0, \mu_{\pm})] \\ &\quad + \frac{g^2 M_{D^0}}{24\pi F_{\pi}^2 M_{D^{*0}}} \Sigma_{D^0 \pi^0 D^0}(E; l, \mu_0), \end{aligned} \quad (42)$$

$$\Gamma_{\pm}^{\mathcal{D}}(E; l) = \Gamma_{[D^{*+} \rightarrow D^+ \gamma]} + \frac{g^2 M_{D^+}}{24\pi F_{\pi}^2 M_{D^{*+}}} \Sigma_{D^+ \pi^0 D^-}(E; l, \mu_{\pm}) + \frac{g^2 M_{D^0}}{12\pi F_{\pi}^2 M_{D^{*+}}} \Sigma_{D^0 \pi^+ D^-}(E; l, \mu_{\pm}). \quad (43)$$

We take the radiative decay widths as constants [10],

$$\Gamma_{[D^{*0} \rightarrow D^0 \gamma]} = 19.5 \text{ keV}, \quad \Gamma_{[D^{*+} \rightarrow D^+ \gamma]} = 1.3 \text{ keV}, \quad (44)$$

while the strong decay width depends on the pion momentum cubed in the rest framework of D^* ,

$$\Sigma_{\alpha\beta\zeta}(E; l, \mu) = \left[2\mu_{\alpha\beta} \left(\sqrt{s} - M_{\alpha} - M_{\beta} - M_{\zeta} - \frac{l^2}{2\mu} \right) \right]^{3/2}, \quad (45)$$

with $\mu_{\alpha\beta} = M_{\alpha}M_{\beta}/(M_{\alpha} + M_{\beta})$. The cut of the square root function in $\Sigma_{\alpha\beta\zeta}(E; l, \mu)$ is defined parallel to the negative imaginary axis on the complex energy plane to ensure a smooth cut crossing in the pole searching procedure [55, 57, 59, 60].

Charged isospin-1 channel

The charged isospin-1 state of $D\bar{D}^*$, named as W_{c1}^{\pm} , can be expressed in flavor space as

$$|W_{c1}^+\rangle = \frac{1}{\sqrt{2}} (|D^+ \bar{D}^{*0}\rangle - |\bar{D}^0 D^{*+}\rangle), \quad |W_{c1}^-\rangle = \frac{1}{\sqrt{2}} (|D^0 D^{*-}\rangle - |D^- D^{*0}\rangle). \quad (46)$$

The pole positions of W_{c1}^{\pm} are determined in a single-channel treatment by using the isospin averaged masses for the charmed mesons, $M_{D^{(*)}} = (M_{D^{(*)0}} + M_{D^{(*)+}})/2$. The potential for the charged isospin-1 state of $D\bar{D}^*$ reads

$$V_+(E_+; p', p) = C_{1X} - \frac{g^2}{12F_{\pi}^2} V_{D^+ \pi^0 \bar{D}^0}^{SS}(E_+; p', p), \quad (47)$$

with $E_+ = \sqrt{s} - M_D - M_{D^*}$. The OPE potential $V_{D^+ \pi^0 \bar{D}^0}^{SS}$ is defined as in Eq. (19). The Green's function in this channel reads

$$G_+(E_+; l) = \frac{1}{E_+ - \frac{l^2}{2\mu_+} + \frac{i}{2}\Gamma_+^{\mathcal{D}}(E_+; l)}, \quad (48)$$

with $\mu_+ = M_D M_{D^*}/(M_D + M_{D^*})$ and the energy-dependent decay width is taken to be the average of those of D^{*0} and D^{*+} ,

$$\Gamma_+^{\mathcal{D}}(E_+; l) = \frac{1}{2} [\Gamma_0^{\mathcal{D}}(E_+; l) + \Gamma_{\pm}^{\mathcal{D}}(E_+; l)]. \quad (49)$$

Riemann sheets

For each channel, the scattering amplitude is in general a multi-valued function of the energy in the c.m. frame since it depends on the on-shell momentum, l_{on} , determined by

$$\frac{1}{G_0(E; l_{\text{on},0})} = 0, \quad \frac{1}{G_{\pm}(E; l_{\text{on},\pm})} = 0, \quad \text{or} \quad \frac{1}{G_+(E_+; l_{\text{on},+})} = 0, \quad (50)$$

for a given E or E_+ . l_{on} has a cut from the threshold, which is on the complex plane because of the finite width of D^* , to infinity. We choose the cut to be a right-hand one.

For the neutral coupled channels, there are two channels and in turn 4 Riemann sheets (RSs), which are labeled with $(\text{sgn}[\text{Im } l_{\text{on},0}], \text{sgn}[\text{Im } l_{\text{on},\pm}])$,

$$\text{RS}(+, +), \text{RS}(-, +), \text{RS}(-, -), \text{RS}(+, -). \quad (51)$$

The $X(3872)$ pole, as a bound state pole, is located on $\text{RS}(+, +)$, while the W_{c1}^0 virtual state pole is located on $\text{RS}(-, -)$. For the charged single channel, there are 2 RSs labeled with $\text{sgn}[\text{Im } l_{\text{on},+}]$,

$$\text{RS}(+), \text{RS}(-), \quad (52)$$

and the W_{c1}^{\pm} virtual state pole is located on $\text{RS}(-)$.

Numerical procedure

With all the singularities in the OPE potential and D^* selfenergy being treated properly, the numerical solution of the integral LSE can be carried out. The integration over momentum l in the numerical LSE is regularized by a sharp cutoff Λ . The momentum integration is performed using the Gauss-Legendre quadrature so that the integral equation becomes a matrix equation. For each channel, the grid points are chosen such that they are much denser in the interval $l \in [0, \Lambda/10]$ than in $l \in [\Lambda/10, \Lambda]$ since the integrand varies more rapidly in the former small interval. Note that the potential never becomes singular on the real- l axis, when $\Gamma_{[D^* \rightarrow D\gamma]} \neq 0$. The determination of the W_{c1} pole positions involves the following sequential steps:

1. Determine the two LECs C_{0X} and C_{1X} by solving the following two equations,

$$T^{-1} \left(-\mathcal{B}_X - i \frac{\Gamma_{X0}}{2} \right) = 0, \quad (53)$$

$$R_{\pm/0} = \lim_{E \rightarrow -\mathcal{B}_X - i\Gamma_{X0}/2} \frac{T_{21}(E)}{T_{11}(E)}, \quad (54)$$

where Γ_{X0} is determined by the iterative procedure mentioned in the main text. The resulting LECs and $X(3872)$ pole position on $\text{RS}(+, +)$ are rechecked so that they indeed satisfy the above two equations.

2. The LECs determined from the first step are used as inputs to solve $T^{-1} \left(-\mathcal{B}_{W_{c1}^0} - i\Gamma_{W_{c1}^0}/2 \right) = 0$ to obtain the pole position of W_{c1}^0 on $\text{RS}(-, -)$ in the neutral coupled channel system, and C_{1X} is also used to solve $T_+^{-1} \left(-\mathcal{B}_{W_{c1}^{\pm}} - i\Gamma_{W_{c1}^{\pm}}/2 \right) = 0$ to obtain the W_{c1}^{\pm} pole position on $\text{RS}(-)$ in the charged single channel system.
3. For a given \mathcal{B}_X in the range of $[0, 180]$ keV, the last two steps are repeated by varying R_X from 0.25 to 0.33 to assess the uncertainties. The outcomes obtained at $R_X = 0.29$ are considered as the central values, while those at $R_X = 0.25$ and 0.33 are treated as the boundaries.
4. The cutoff dependence of the W_{c1} pole positions is checked numerically by varying Λ from 0.5 to 1 GeV, and the pole positions in E exhibit a minor change of less than 5%, which is indeed of $\mathcal{O}(Q^2/\Lambda^2)$.

Results in the pionless theory

In the pionless theory, the LSE for the $(D\bar{D}^*)_0^{[C=+]}-(D\bar{D}^*)_{\pm}^{[C=+]}$ coupled channels in Eq. (10) is reduced to

$$T(E) = V_{\text{ct}} + V_{\text{ct}}J(E)T(E) = \frac{1}{V_{\text{ct}}^{-1} - J(E)} \quad (55)$$

where

$$J(E) = \begin{pmatrix} -\frac{\mu_0\Lambda}{\pi^2} - \frac{i\mu_0}{2\pi}k_0 & 0 \\ 0 & -\frac{\mu_{\pm}\Lambda}{\pi^2} - \frac{i\mu_{\pm}}{2\pi}k_{\pm} \end{pmatrix} \equiv \begin{pmatrix} d_0^{\Lambda} - \frac{i\mu_0}{2\pi}k_0 & 0 \\ 0 & d_{\pm}^{\Lambda} - \frac{i\mu_{\pm}}{2\pi}k_{\pm} \end{pmatrix}, \quad (56)$$

with

$$k_0 = \sqrt{2\mu_0 E + i\mu_0 \Gamma_{D^{*0}}}, \quad k_{\pm} = \sqrt{2\mu_{\pm}(E - \Delta) + i\mu_{\pm} \Gamma_{D^{*+}}}, \quad (57)$$

the on-shell c.m. momenta in $D^0\bar{D}^{*0}$ and D^+D^{*-} channels, respectively. Here, $\Gamma_{D^{*0}} = 55.3$ keV [61] and $\Gamma_{D^{*+}} = 83.4$ keV [10] are taken to be constants.

The cutoff dependence can be fully absorbed by V_{ct} when isospin breaking is neglected in the short-distance contributions, $d_0^{\Lambda} = d_{\pm}^{\Lambda} \equiv d^{\Lambda}$, and hence

$$T^{-1}(E) = V_{\text{ct}}^{-1} - J(E) = (V_{\text{ct}}^R)^{-1} - J^R(E), \quad (58)$$

with

$$V_{\text{ct}}^R = \frac{1}{2} \begin{pmatrix} C_{0X}^R + C_{1X}^R & C_{0X}^R - C_{1X}^R \\ C_{0X}^R - C_{1X}^R & C_{0X}^R + C_{1X}^R \end{pmatrix}, \quad \text{and} \quad J^R(E) = \begin{pmatrix} -\frac{i\mu_0}{2\pi}k_0 & 0 \\ 0 & -\frac{i\mu_{\pm}}{2\pi}k_{\pm} \end{pmatrix}. \quad (59)$$

The bare and renormalized LECs are related by

$$C_{0X}^{-1} = \frac{1 + (C_{0X}^R + C_{1X}^R)d^{\Lambda} + C_{0X}^R C_{1X}^R (d^{\Lambda})^2}{C_{0X}^R + C_{0X}^R C_{1X}^R d^{\Lambda}}, \quad C_{1X}^{-1} = \frac{1 + (C_{0X}^R + C_{1X}^R)d^{\Lambda} + C_{0X}^R C_{1X}^R (d^{\Lambda})^2}{C_{1X}^R + C_{0X}^R C_{1X}^R d^{\Lambda}}. \quad (60)$$

Using the $X(3872)$ binding energy and the decay ratio R_X as inputs, C_{0X}^R and C_{1X}^R can be solved as

$$C_{0X}^R = \frac{[1 + R_{\pm/0}][J_1^R - R_{\pm/0}J_2^R]}{(J_1^R)^2 - R_{\pm/0}^2(J_2^R)^2}|_{E=-\mathcal{B}_X}, \quad C_{1X}^R = \frac{[1 - R_{\pm/0}][J_1^R + R_{\pm/0}J_2^R]}{(J_1^R)^2 - R_{\pm/0}^2(J_2^R)^2}|_{E=-\mathcal{B}_X}, \quad (61)$$

and as functions of \mathcal{B}_X , shown in the left panel of Fig. 7.

For the charged isospin-1 single channel, the LSE reads

$$T_+(E) = \frac{1}{C_{1X}^{-1} - J_+(E)} = \frac{1}{(C_{1X}^R)^{-1} - J_+^R(E)}, \quad (62)$$

where

$$J_+ = -\frac{\mu_+\Lambda}{\pi^2} - \frac{i\mu_+}{2\pi}k_+ \equiv d_+^{\Lambda} - \frac{i\mu_+}{2\pi}k_+, \quad J_+^R = -\frac{i\mu_+}{2\pi}k_+, \quad (63)$$

with $k_+ = \sqrt{2\mu_+ E + i\mu_+ \Gamma_{D^*}}$, and $\Gamma_{D^*} = (\Gamma_{D^{*0}} + \Gamma_{D^{*+}})/2$, and again short-distance isospin breaking is neglected such that $d_+^{\Lambda} = d^{\Lambda}$.

Using the determined C_{0X}^R and C_{1X}^R , we predict the W_{c1}^0 and W_{c1}^{\pm} pole positions as functions of \mathcal{B}_X , shown in the right panel of Fig. 7. Comparing them with the results with fully dynamical pions in Fig. 3, one sees that the real parts are similar while the imaginary parts differ significantly. This is expected as the imaginary parts are dominated by the $D\bar{D}\pi$ cuts.

Setting $\mathcal{B}_X = 180$ keV, the predicted lineshape of the $(D\bar{D}^*)_0^{[C=+]}-(D\bar{D}^*)_{\pm}^{[C=+]}$ coupled-channel T matrix and the isovector $D^+\bar{D}^{*0}$ single-channel scattering T -matrix elements are illustrated in Fig. 8. The contact term for the $J_I^{PC} = 2_1^{++}$ $D^*\bar{D}^*$ system is also C_{1X}^R . Using the determined values of C_{1X}^R in Fig. 7, the W_{c2} mass is predicted to be $4010.4_{-3.5}^{+2.2}$ MeV from the pole position of the $D^*\bar{D}^*$ single channel T matrix, where the isospin-averaged mass of D^* is taken.

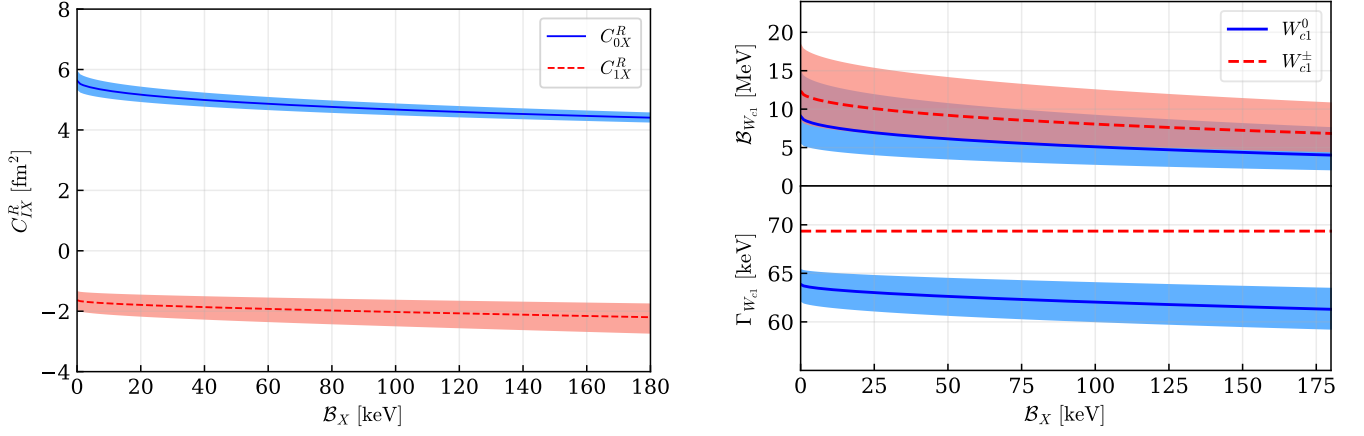


FIG. 7. Left: Renormalized C_{0X}^R and C_{1X}^R as functions of B_X . Right: Dependence of the predicted W_{c1} virtual state pole position on the input $X(3872)$ binding energy in the pionless theory. The bands are from the uncertainty in Eq. (8). Upper: real part of the pole position with respect to the $D^0\bar{D}^{*0}$ (for W_{c1}^0) or $D^0\bar{D}^{*-}$ (for W_{c1}^\pm) threshold. Lower: twice the magnitude of the imaginary part of the W_{c1} pole position. The bands are due to the uncertainty in Eq. (8).

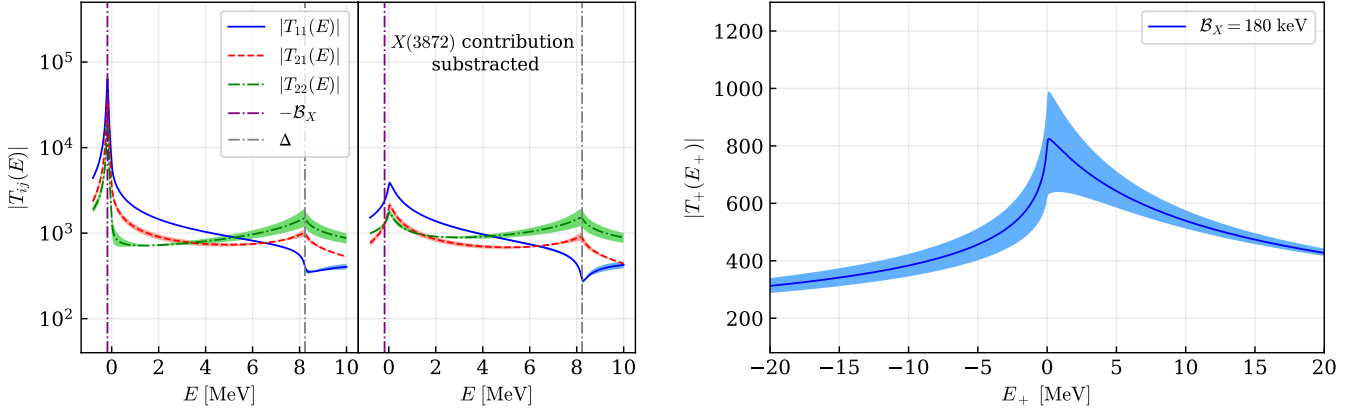


FIG. 8. Left: Line shapes of the S -wave $D^0\bar{D}^{*0}-D^+D^{*-}$ scattering T -matrix elements in the pionless theory, where the left and right parts are for the full T -matrix elements and the T -matrix elements with the $X(3872)$ pole contribution subtracted, respectively. Right: Line shape of the single-channel $D^+\bar{D}^{*0}$ scattering T -matrix element, with E_+ defined relative to the $D^+\bar{D}^{*0}$ threshold. Here B_X is set to 180 keV and the uncertainty is from Eq. (8).